PERGAMON

International Journal of Solids and Structures 38 (2001) 7501–7524

INTERNATIONAL JOURNAL OF SOLIDS and STRUCTURES

www.elsevier.com/locate/ijsolstr

Sliding on cracks with non-uniform frictional characteristics

Larissa Gorbatikh [a], Boris Nuller [b], Mark Kachanov [a,*]

[a] *Department of Mechanical Engineering, Tufts University, 204 Anderson Hall, Medford, MA 02155, USA*
[b] *Department of Mathematics, Academy of Forest Technologies, St.-Petersburg, 195220 Russia*

Received 18 May 2000

Abstract

A crack that undergoes partial frictional sliding under compression and shear is analyzed. The frictional resistance is assumed to be non-uniform along the sliding contact. This non-uniformity may be due to variability of the coefficient of friction or due to variability of the normal traction along the crack (that may be caused by some external factors). Sliding, generally, starts at point(s) of low frictional resistance and may propagate along the crack as the applied loads are changed. This process and its sensitivity to the profile of the frictional resistance are analyzed. We also analyze the case when "open" (traction free) intervals along the crack are present; such intervals model the situations when a part of the material "fell off" and contact between the crack faces is partially lost.

Keywords: Friction; Crack; Sliding

1. Introduction

The problem of frictionally sliding cracks is relevant for a number of applications, particularly geomechanical ones, where the stress conditions are predominantly compressive, with substantially different principal stresses. If shear tractions are sufficiently high, they may overcome the frictional resistance and initiate sliding. If the frictional resistance is uniform along the sliding contact, then sliding occurs at all points of the surface simultaneously. However, this assumption may be inadequate for many applications, like sliding processes along geological faults (Pollard, 1980; Cooke, 1997; Schultz, 1999).

The present work analyzes initiation and propagation of sliding zones on one or several collinear two-dimensional cracks under increasing applied shear load. Frictional resistance is assumed to be non-uniform along the frictional contact. This non-uniformity may be due to variability of the coefficient of friction (local lubrications or a loss of lubricant) or due to variability of the normal traction along the crack (caused by some external factors, for example, local fluid pressures). We also analyze the distribution of displacement discontinuity (the accumulated slip) along the crack.

* Corresponding author. Tel.: +1-617-627-3318; fax: +1-617-627-3058.
E-mail address: mark.kachanov@tufts.edu (M. Kachanov).

0020-7683/01/$ - see front matter
PII: S0020-7683(01)00011-7

The crack may experience three different regimes along its surface: intervals undergoing frictional sliding, "open" (traction free) intervals and "locked" intervals. Open intervals model the situations when a part of the material "fell off" and contact between the crack faces is partially lost. They are taken as fixed intervals that are not caused by any loads. We mention, in this connection, a somewhat different problem analyzed by Mendelsohn and Whang (1988) and Dundurs and Comninou (1979, 1981): the sliding line contained an opening due to application of local "prying" forces or moments. The locked intervals differ from the virgin continuous material by the requirement that stress intensity factors at their endpoints are zeros.

Sliding starts at point(s) of minimal frictional resistance and then propagates, as the applied shear load is increased, until it covers the entire crack length. The propagation of sliding is determined by the condition for the stress intensity factor: $K_{\mathrm{II}} = 0$ at the ends of the sliding interval(s). This condition allows one to find locations of the endpoints of the sliding zone(s) as functions of applied loads. We study the evolution of such zones under changing loads, sensitivity of the process to various physical factors (the shape of local maxima/minima of the frictional resistance, the case when the sliding zone reaches one of the crack tips), the enhancing effect of interaction between several sliding zones and the influence of the open intervals on the sliding process.

In two special cases, when the frictional resistance profile has one local minimum, either in the form of stepwise constant discontinuity or in the form of a triangle, the problem was analyzed by Weertman (1964) and Olsson (1984), correspondingly. We also mention the work of Comninou and Dundurs (1983) where the propagation of sliding from a local minimum of frictional resistance was considered, in a more general case of sliding along the interface of two different materials. Their analysis, however, was restricted to the case of only one local minimum of the frictional resistance, with actual results given for the parabolic shape of the minimum. The present analysis applies to the frictional resistance profile of a general shape that may have several extremums; it covers the above mentioned situations as special cases.

2. Formulation of the problem

We consider an infinite two-dimensional solid with a crack $(-l,\ l)$ along the x-axis. Stresses at infinity (applied loads) are $\sigma_{yy}^{\infty} < 0$ (compressive) and $\sigma_{xy}^{\infty} > 0$. The frictional resistance is assumed to be variable along the crack: $\tau = \tau(x)$. We emphasize that, although the frictional resistance may, as a special case, be modeled by Coulomb's law $\tau(x) = -\mu(x)\,\sigma_{yy} + c(x)$ (where $\mu(x)$ and $c(x)$ are the coefficients of friction and cohesion, respectively), such a modeling is not essential for the present analysis. The sliding process may start at points of local minima of $\tau(x)$ and then propagate along the crack, as applied loads are changed. This process is studied in the present work.

As mentioned above, the crack may experience three different regimes along its surface: intervals undergoing frictional sliding, locked intervals and open (traction free) intervals (schematically shown in Fig. 1). These regimes are defined by the following boundary conditions (brackets [ ] denote discontinuities of the corresponding quantities):

(1) Along the set L_1 of *frictionally sliding* intervals

$$\left|\sigma_{xy}\right| = \tau(x), \quad \left[u_y\right] = 0, \quad \left[\sigma_{xy}\right] = \left[\sigma_{yy}\right] = 0 \qquad \text{for } x \in L_1 \tag{2.1a}$$

subject to the inequality

$$\sigma_{yy} < 0 \quad \text{for } x \in L_1 \tag{2.1b}$$

(2) Along the set L_2 of *locked* intervals

$$[u_x] = \left[u_y\right] = 0, \quad \left[\sigma_{xy}\right] = \left[\sigma_{yy}\right] = 0 \qquad \text{for } x \in L_2 \tag{2.2a}$$

subject to the inequalities

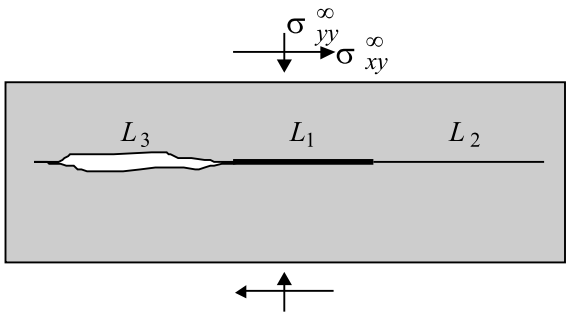

Fig. 1. Crack line consisting of a sliding interval L_1, a locked interval L_2 and an open interval L_3 (each of the intervals may comprise of several subintervals).

$$\sigma_{yy} < 0, \qquad \left|\sigma_{xy}\right| < \tau(x) \quad \text{for } x \in L_2 \tag{2.2b}$$

(It is assumed that $\sigma_{xy} > 0$ in the text to follow, so that the sign || will be omitted.)

(3) Along the set L_3 of fixed *open (traction free)* intervals

$$\sigma_{xy} = \sigma_{yy} = 0 \quad \text{for } x \in L_3 \tag{2.3a}$$

Note that the method developed in the present work actually covers a more general case when an arbitrary distribution of equal and opposite tractions is applied on L_3:

$$\sigma_{xy} = \tau_*(x), \quad \sigma_{yy} = \sigma_*(x) \qquad \text{for } x \in L_3 \tag{2.3b}$$

Such a generalization allows for physically interesting situations, for example, the case of fluid pressure applied along L_3.

The condition of non-overlapping of crack faces should also be imposed:

$$\left[u_y\right] \geqslant 0 \quad \text{for } x \in L_3 \tag{2.4a}$$

In a more general case, when a certain finite initial crack opening $\Delta(x)$ along L_3 is present, (2.4a) can be relaxed to

$$\Delta + \left[u_y\right] \geqslant 0 \tag{2.4b}$$

The points that separate the intervals of sliding L_1 from the locked intervals L_2 are determined from the following condition for stress intensity factor (SIF):

$$K_{\mathrm{II}} = 0 \tag{2.5a}$$

Indeed, $K_{\mathrm{II}} \neq 0$ at the end point of L_1 would have generated a singularity of shear stress σ_{xy} in L_2, thus producing sliding there. Note that the condition (2.5a) is necessary, but not sufficient for the determination of the endpoints of L_1 – the inequalities (2.2b) have to be verified.

If an endpoint of L_1 coincides with one of the crack tips $x = \pm l$ then condition (2.5a) should be replaced by

$$K_{\mathrm{II}} < K_{\mathrm{IIC}} \tag{2.5b}$$

where K_{IIC} is a material constant representing the resistance to shear fracture.

In the present paper, the analysis is restricted to the case of the "monotonic" propagation of sliding, in the sense that the intervals where sliding has been started, continue to slide as the applied loads change. Extension of the analysis to the cyclic loadings will be given in a follow-up manuscript.

3. General solution in absence of open intervals

We first consider the case when there are no open (traction free) intervals L_3 and the crack line comprises interval(s) L_1 of frictional sliding, possibly alternating with locked intervals L_2 (Fig. 2). Note that $\sigma_{yy} = \sigma_{yy}^{\infty}$ on the entire crack length $L_1 \cup L_2$ (so that, if Coulomb's law is assumed, then $\sigma_{xy} = \tau(x) = -\mu(x)\,\sigma_{yy}^{\infty} + c(x)$ along L_1).

Using the stress superposition (Fig. 2), we reduce the problem, at each stage of loading, to the linear elastic one, with shear traction $\sigma_{xy} = \sigma_{xy}^{\infty} - \tau(x)$ on L_1. Note that, as follows from the analysis to follow, $\sigma_{xy} < 0$ in the parts of L_1 that are adjacent to the endpoints of L_1 and, generally, $\sigma_{xy} > 0$ in its central part (unless sliding zone L_1 has developed as a result of coalescence of two sliding zones, in which case σ_{xy} may be negative along the former ligament). As far as the locked intervals L_2 are concerned, the difference $\sigma_{xy}^{\infty} - \tau(x)$ is negative there (otherwise, sliding would have occurred within L_2).

Following the usual formalism of two-dimensional elasticity, the solution is sought in terms of Kolosov–Muskhelishvili's potentials:

$$2G\left(u_x + \mathrm{i}u_y\right)' = \kappa\Phi(z) - \Phi(\bar{z}) - (z-\bar{z})\overline{\Phi'(z)} \tag{3.1a}$$

$$\sigma_{yy} - \mathrm{i}\sigma_{xy} = \Phi(z) + \Phi(\bar{z}) + (z-\bar{z})\overline{\Phi'(z)} \tag{3.1b}$$

where G is the shear modulus, $\kappa = 3 - 4\nu$ for plane strain and $\kappa = (3-\nu)/(1+\nu)$ for plane stress (ν is Poisson's ratio). Functions $\Phi(z)$, as well as $\overline{\Phi}(z)$ (of complex variable $z = x + \mathrm{i}y$) defined by the relation $\overline{\Phi}(z) \equiv \overline{\Phi(\bar{z})}$, are piecewise analytic, with L_1 and L_3 being the discontinuity lines.

Assuming that, in the general case, the sliding zone L_1 comprises n sliding subintervals $L_1^{(k)}$, with yet unknown endpoints a_k, b_k (alternating with locked subintervals of L_2), we have the following expression for the complex potential $\Phi(z)$ (see, e.g. Muskhelishvili, 1953):

$$\Phi(z) = \frac{1}{2\pi X(z)} \int_{L_1} \frac{X(t)\,\sigma_{xy}(t)\,\mathrm{d}t}{t-z} + \mathrm{i}\frac{P_n(z)}{X(z)} \tag{3.2}$$

where

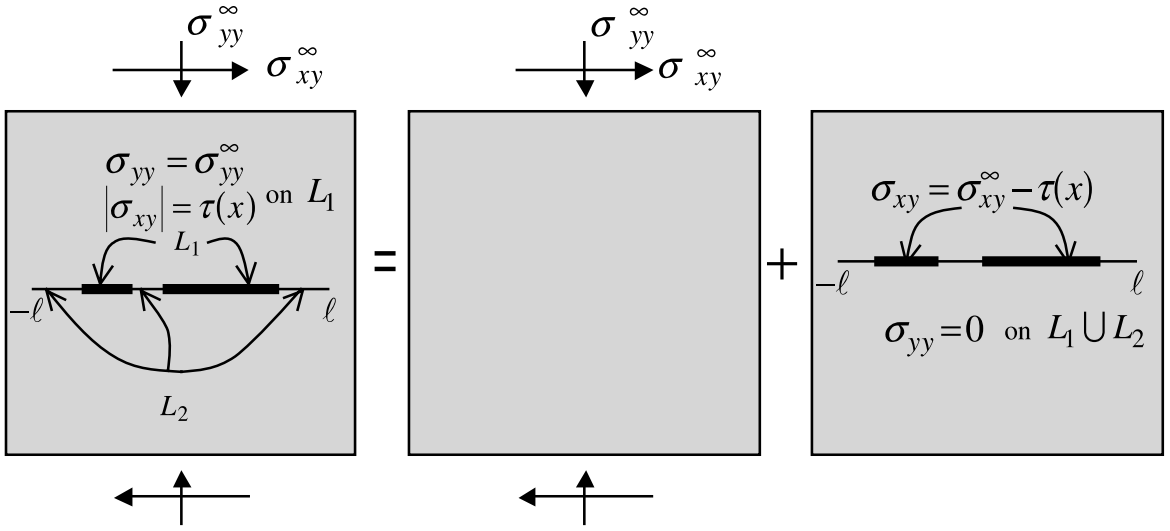

Fig. 2. Stress superposition for a crack comprising sliding interval L_1 and locked interval L_2.

$$X(z) = \sqrt{(z-a_1)(z-b_1)\cdots(z-a_n)(z-b_n)} \tag{3.3}$$

with the branch chosen in such a way that $z^{-n}X(z) \to 1$ as $z \to \infty$ (hence $X^+(t) = X(t)$ and $X^-(t) = -X(t)$ on L_1, where t is the coordinate along x-axis) and $P_n(z)$ is a polynomial of degree $\leqslant n$:

$$P_n(z) = C_0 z^n + C_1 z^{n-1} + \cdots + C_n \tag{3.4}$$

with real coefficients to be found from n conditions of uniqueness of displacements at points a_k and b_k:

$$\oint_{\Lambda_1^{(k)}} \Phi(z)\,\mathrm{d}z = 0 \quad (k = 1, \ldots, n) \tag{3.5}$$

where $\Lambda_1^{(k)}$ are closed contours encircling $L_1^{(k)}$.

We now determine the stress intensity factors entering the condition (2.5a):

$$K_{\mathrm{II}}(z_k) = \begin{cases} \lim_{z\to z_k} \sqrt{z-z_k}\,\Phi(z), & \text{for } z_k = b_k \\ \mathrm{i}\lim_{z\to z_k} \sqrt{z-z_k}\,\Phi(z), & \text{for } z_k = a_k \end{cases} \tag{3.6}$$

or, after some algebra,

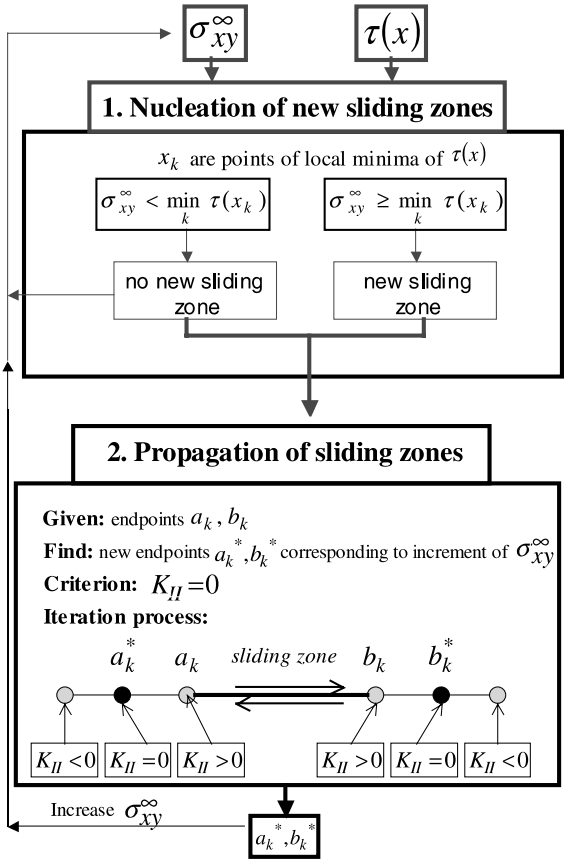

Fig. 3. Iterative procedure of finding endpoints of the sliding zone(s).

$$K(z_k) = \frac{F(z_k) + P_n(z_k)}{\sqrt{(b_k - a_k)\prod_{i\neq k}(z_k - a_i)(z_k - b_i)}} \tag{3.7}$$

In the expression above $F(z_k) = \lim_{z\to z_k} F(z)$, where

$$F(z) = \frac{1}{2\pi i}\int_{L_1} \frac{X(t)p(t)\,dt}{t - z}$$

is Cauchy's integral and the coefficients of $P_n(z)$ are determined from the following system of n linear algebraic equations:

$$2\int_{L_1^{(k)}} \frac{C_1 t^{n-1} + \cdots + C_n}{X(t)}\,dt + \frac{1}{\pi i}\int_{L_1^{(k)}} \frac{1}{X(t)}\int_{L_1} \frac{X(\xi)\,\sigma_{xy}(\xi)\,d\xi}{\xi - t}\,dt = 0, \quad k = 1, \ldots, n \tag{3.8}$$

where second integral has a non-integrable singularity along $L_1^{(k)}$ when $L_1 = L_1^{(k)}$ and has to be understood in the principal value sense.

We now outline the procedure of analysis of the sliding process (Fig. 3). Sliding starts at the point(s) x of local minima of frictional resistance $\tau(x)$. As the applied shear load σ_{xy}^{∞} is increased, sliding zone(s) propagate. The criterion for locating the new endpoints of the sliding zones is that the stress intensity factors at the endpoints have to be equal to zero: $K_{II} = 0$. In the case of only one sliding zone, this condition yields two non-linear algebraic equations for the endpoints' coordinates. In the case of N sliding zones, we obtain a system of $2N$ coupled algebraic equations. This system is solved by iterations, with the solution for non-interacting zones being the first approximation.

As far as the basic solution for one sliding zone is concerned, in the case of piecewise constant minimum it can be constructed exactly (see Section 4.1); for more complex profiles of the frictional resistance, the solution of Section 4.2 for the asymmetric minimum provides a good approximation.

4. Analysis of various factors affecting the propagation of sliding zones

We analyze the influence of the profile of frictional resistance $\tau(x)$ on the initiation and propagation of the sliding zones, as the applied shear traction (or driving force) is increased. (In the simplest case, when $\tau(x) \equiv \tau_0 = \text{const}$, sliding occurs along the entire crack line when the applied shear load reaches the value of the frictional resistance: $\sigma_{xy}^{\infty} - \tau_0 = 0$.)

4.1. Piecewise constant profile of $\tau(x)$ with a local minimum

We consider the case of piecewise constant distribution of $\tau(x)$ with one local minimum:

$$\tau(x) = \begin{cases} \tau_1, & a < x < b \\ \tau_2, & b < x < l \\ \tau_3, & -l < x < a \end{cases} \tag{4.1}$$

where $\tau_1 \leqslant \tau_2 \leqslant \tau_3$. This case models, for example, the situation when Coulomb's law is assumed, with friction coefficient $\mu(x)$ being piecewise constant and cohesion coefficient $c(x)$ being constant. In this case, the problem of propagation of the sliding zone (in terms of applied loads) can be solved in closed form and in elementary functions.

The entire crack is locked until the applied load reaches a critical level: $\sigma_{xy}^{\infty} = \tau_1$ at the point(s) of the lowest frictional resistance. At this point, sliding starts in the interval $a < x < b$ and, as σ_{xy}^{∞} is increased, sliding spreads into the adjacent intervals $(a - \varepsilon_3, a)$ and $(b, b + \varepsilon_2)$. In the text to follow, we derive ex-

pressions for ε_2 and ε_3 as functions of σ_{xy}^{∞}, from the condition that SIF $K_{\mathrm{II}} = 0$ at the ends of the sliding zone $(a - \varepsilon_3,\ b + \varepsilon_2)$.

The condition $K_{\mathrm{II}} = 0$ translates into the following two equations:

$$K_{\mathrm{II}} \left\{ \begin{matrix} a - \varepsilon_3 \\ b + \varepsilon_2 \end{matrix} \right\} = -\sqrt{\frac{2}{\pi(b + \varepsilon_2 - a + \varepsilon_3)}} \int_{a-\varepsilon_3}^{b+\varepsilon_2} \sigma_{xy}(x) \left\{ \frac{b + \varepsilon_2 - x}{x - a + \varepsilon_3} \right\}^{\pm(1/2)} \mathrm{d}x = 0 \tag{4.2}$$

where

$$\sigma_{xy}(x) = \sigma_{xy}^{\infty} - \tau(x). \tag{4.3}$$

Substituting Eq. (4.3) into Eq. (4.2) and calculating the integrals one obtains

$$\begin{aligned} K_{\mathrm{II}} \left\{ \begin{matrix} a - \varepsilon_3 \\ b + \varepsilon_2 \end{matrix} \right\} = \sqrt{\frac{b - a + \varepsilon_2 + \varepsilon_3}{2\pi}} \Bigg\{ \pi\sigma_{xy}^{\infty} - \Bigg[(\tau_2 - \tau_1) \arcsin \frac{a - b + \varepsilon_2 - \varepsilon_3}{b - a + \varepsilon_2 + \varepsilon_3} \\ - (\tau_3 - \tau_1) \arcsin \frac{b - a + \varepsilon_2 - \varepsilon_3}{b - a + \varepsilon_2 + \varepsilon_3} + (\pi/2)(\tau_2 + \tau_3) \Bigg] \Bigg\} \\ \pm \sqrt{\frac{2}{\pi(b - a + \varepsilon_2 + \varepsilon_3)}} \Big[(\tau_2 - \tau_1) \sqrt{(b - a + \varepsilon_3)\varepsilon_2} - (\tau_3 - \tau_1) \sqrt{(b - a + \varepsilon_2)\varepsilon_3} \Big] \end{aligned} \tag{4.4}$$

Equating $K_{\mathrm{II}} \left\{ \begin{matrix} a - \varepsilon_3 \\ b + \varepsilon_2 \end{matrix} \right\}$ to zero yields two equations; adding and subtracting them leads to the following two equations for ε_2 and ε_3:

$$\begin{aligned} \sigma_{xy}^{\infty} &= \frac{\tau_2 + \tau_3}{2} + \frac{\tau_2 - \tau_1}{\pi} \arcsin \frac{s(1 - \alpha_2^2) - 1}{s(1 + \alpha_2)^2 - 1} - \frac{\tau_3 - \tau_1}{\pi} \arcsin \frac{s(1 + \alpha_2)^2 - 2\alpha_2 - 1}{s(1 + \alpha_2)^2 - 1} \\ \alpha_3 &= s\alpha_2 + s - 1 \end{aligned} \tag{4.5}$$

where

$$s = \left(\frac{\tau_3 - \tau_1}{\tau_2 - \tau_1} \right)^2 \quad \text{and} \quad \alpha_k = (b - a)\varepsilon_k^{-1}.$$

Numerical solution of Eq. (4.5) is illustrated in Fig. 4 (for the case when $a = -0.2$, $b = 0.2$, $\tau_1 = 0.5\tau_0$, $\tau_2 = \tau_0$, $\tau_3 = 1.5\tau_0$). As sliding starts in the interval (a, b) of reduced frictional resistance $\tau(x)$, it propagates at both ends. However, the rates of propagation at the left and the right endpoints are different; they are interrelated through parameter s.

An interesting observation is that Eq. (4.5) do not contain any reference to the length $2l$ of the *entire* crack, up to the point when the sliding zone reaches one of the tips $-l, l$ of the crack. The load σ_{xy}^{∞} at which the sliding zone reaches the right tip of the crack is found from Eq. (4.5):

$$\sigma_{xy}^{\infty} = \frac{\tau_2 + \tau_3}{2} + \frac{\tau_2 - \tau_1}{\pi} \arcsin \frac{s(1 - \alpha^2) - 1}{s(1 + \alpha)^2 - 1} - \frac{\tau_3 - \tau_1}{\pi} \arcsin \frac{s(1 + \alpha)^2 - 2\alpha - 1}{s(1 + \alpha)^2 - 1} \tag{4.6}$$

where $\alpha = (b - a)/(l - b)$. At this point, condition $K_{\mathrm{II}} = 0$ at the right tip should be changed to $K_{\mathrm{II}} < K_{\mathrm{IIC}}$ and the propagation continues only on the left. At this stage, the equation for ε_3, similar to Eq. (4.5), can be derived:

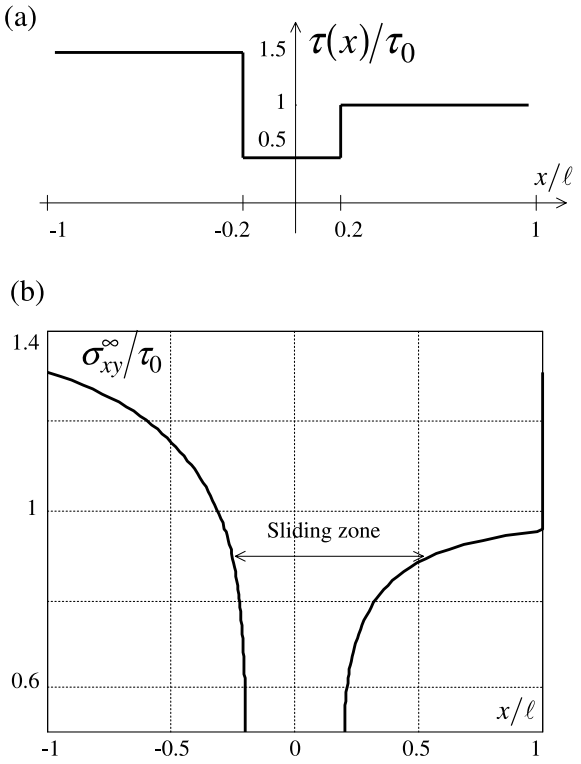

Fig. 4. Propagation of the sliding zone in the case of piecewise constant frictional resistance, as σ^{∞}_{xy} increases.

$$\sigma^{\infty}_{xy}+\frac{\tau_2-\tau_1}{\pi}\left(\frac{2\sqrt{(b-a+\varepsilon_3)(l-b)}}{(l-a+\varepsilon_3)}-\arcsin\frac{l+a-2b-\varepsilon_3}{l-a+\varepsilon_3}\right)$$
$$-\frac{\tau_3-\tau_1}{\pi}\left(\frac{2\sqrt{\varepsilon_3(l-a)}}{l-a+\varepsilon_3}-\arcsin\frac{l-a-\varepsilon_3}{l-a+\varepsilon_3}\right)-\frac{\tau_2+\tau_3}{2}=0 \tag{4.7}$$

At $\varepsilon_3 = l + a$ (the left tip $-l$ is reached), this formulae gives the corresponding load σ^{∞}_{xy}:

$$\sigma^{\infty}_{xy}+\frac{\tau_2-\tau_1}{\pi}\left(\arcsin\frac{b}{l}+\sqrt{1-\frac{b^2}{l^2}}\right)-\frac{\tau_3-\tau_1}{\pi}\left(\arcsin\frac{a}{l}+\sqrt{1-\frac{a^2}{l^2}}\right)-\frac{\tau_2+\tau_3}{2}=0 \tag{4.8}$$

In the symmetric case $\tau_2 = \tau_3$, we have $\varepsilon_3 = \varepsilon_2 \equiv \varepsilon$, with the following solution for the length ε:

$$\varepsilon=\frac{b-a}{2}\left(\frac{1}{\sin Q}-1\right)\quad\text{where } Q=-\frac{\pi(\sigma^{\infty}_{xy}-\tau_2)}{2(\tau_2-\tau_1)} \tag{4.9}$$

that recovers the result of Weertman (1964).

4.2. Piecewise linear profile of $\tau(x)$ with a local minimum

We now consider the following profile of frictional resistance $\tau(x)$ (Fig. 5a):

$$\tau(x)=\begin{cases}\tau_1 & a<x<b\\ p_2+q_2x & b<x<\ell\\ p_3+q_3x & -\ell<x<a\end{cases} \tag{4.10}$$

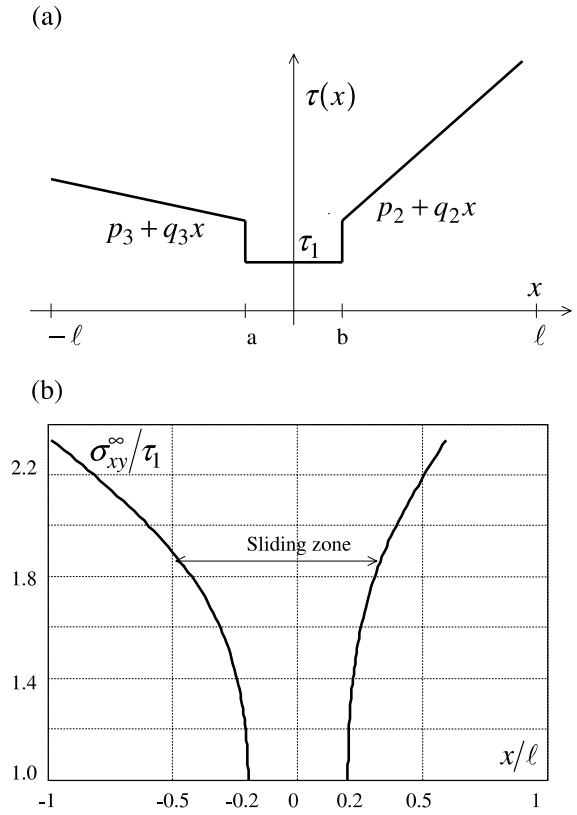

Fig. 5. The case of asymmetric frictional resistance (with a local drop). Propagation of the sliding zone as σ^{∞}_{xy} increases ($p_2 = p_3 = 0.9$, $q_3 = -0.5$ and $q_2 = 0.75$).

This case is of importance, since it may be used, as an approximation, for many other profiles of frictional resistance containing a local minimum. Indeed, as shown in the text to follow (Section 4.3), after a certain vicinity of the local minimum has slid, effect on the subsequent sliding may be modeled, with good accuracy, by replacing it by an interval of piecewise constant, "flat" minimum, of the magnitude that preserves the average of the drop over this vicinity. The problem considered here may be used as the basic building block for an iteration process in the case of several interacting sliding zones and complex profiles of the frictional resistance.

As σ^{∞}_{xy} is increased, sliding spreads into the adjacent intervals (b, ε_2), (ε_3, a) and new endpoints of the sliding zone $(\varepsilon_3, \varepsilon_2)$ can be found from the condition $K_{\mathrm{II}} = 0$.

This condition translates into two non-linear algebraic equations for ε_2 and ε_3:

$$\begin{aligned} &q_3\left(\frac{\pi}{2} - \arcsin\frac{-2a + \varepsilon_3 + \varepsilon_2}{\varepsilon_2 - \varepsilon_3}\right) + q_2\left(\frac{\pi}{2} + \arcsin\frac{-2b + \varepsilon_3 + \varepsilon_2}{\varepsilon_2 - \varepsilon_3}\right) = 0 \\ &F(a, p_3, q_3, 0) - F(b, p_2, q_2, 1) = 0 \end{aligned} \tag{4.11}$$

where

$$F(\xi,p,q,k)=\sqrt{\varepsilon_2-\xi}\sqrt{\xi-\varepsilon_3}\left(\sigma_{xy}^{\infty}-p-q\xi+q\frac{2\xi-\varepsilon_3-\varepsilon_2}{4}\right)$$
$$+\left(-\frac{\varepsilon_3-\varepsilon_2}{2}\left(\sigma_{xy}^{\infty}-p\right)-q\frac{(\varepsilon_3-\varepsilon_2)^2}{8}-q\frac{\varepsilon_3^2-\varepsilon_2^2}{4}\right)\left(-\arcsin\frac{-2\xi+\varepsilon_3+\varepsilon_2}{\varepsilon_3-\varepsilon_2}+(-1)^k\frac{\pi}{2}\right)$$
$$-\left(\sigma_{xy}^{\infty}-\tau_1\right)\left(\sqrt{\varepsilon_3-\xi}\sqrt{\xi-\varepsilon_2}-\frac{\varepsilon_3-\varepsilon_2}{2}\arcsin\frac{-2\xi+\varepsilon_3+\varepsilon_2}{\varepsilon_3-\varepsilon_2}\right)$$
$$+q\frac{(\varepsilon_3-\varepsilon_2)^2}{4}\sqrt{1-\left(\frac{-2\xi+\varepsilon_3+\varepsilon_2}{\varepsilon_3-\varepsilon_2}\right)^2}$$

These two equations can be solved, for example, by iterations. The solution (propagation of the sliding zone) is illustrated in Fig. 5b.

4.3. Sensitivity of the sliding process to the profile of frictional resistance

The available information on frictional resistance $\tau(x)$, as a function of a point on the crack (“frictional resistance profile”) is, at best, approximate. It is important, therefore, to examine the sensitivity of the sliding process to the “details” of the profile.

The following observations, made on the basis of case studies performed in the framework of our formulation, can be made.

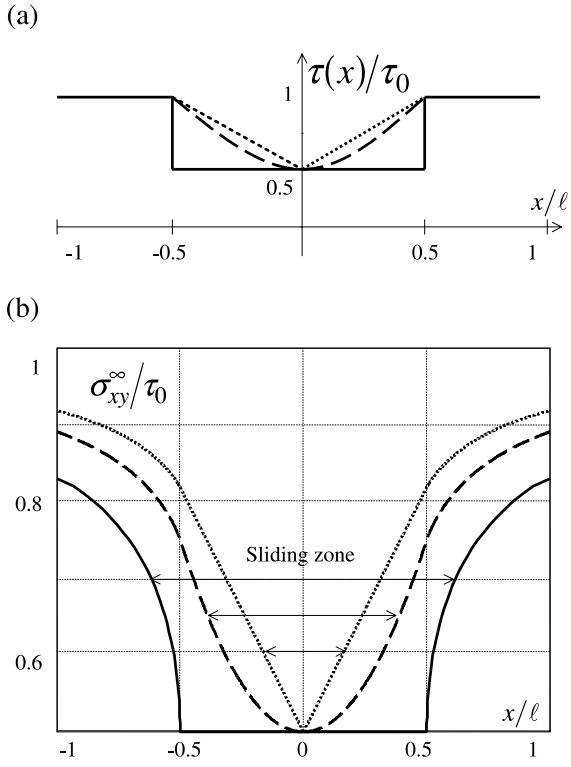

Fig. 6. Sensitivity of the sliding process to the exact profile of frictional resistance in the case of local minimum of $\tau(x)$. Propagation of sliding for three different profiles of $\tau(x)$.

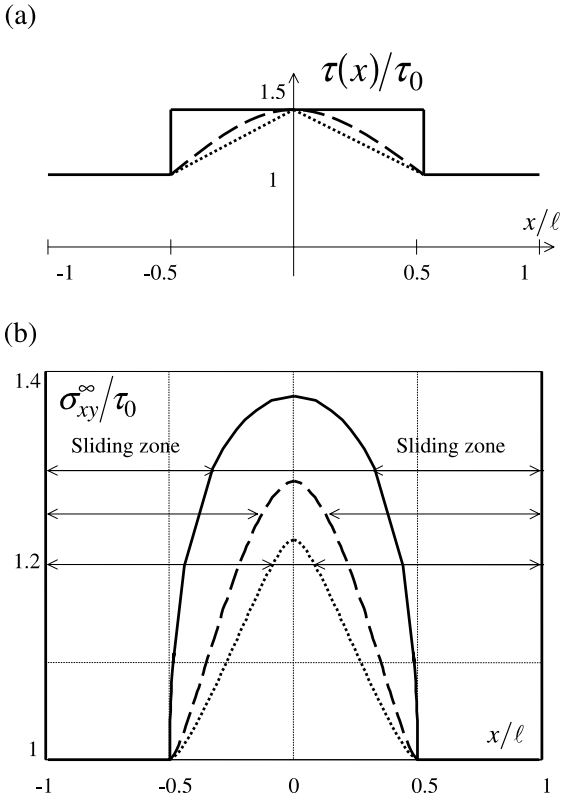

Fig. 7. Sensitivity of the sliding process to the exact profile of frictional resistance in the case of local maximum of $\tau(x)$. Propagation of sliding for three different profiles of $\tau(x)$.

(A) As the applied shear loading increases, the rate of propagation of the sliding zone is initially sensitive to the local details of the frictional resistance profile.

(B) However, the sensitivity to these details within the zone of local reduction of $\tau(x)$ that has already been slid is quickly lost: the "memory" of the resistance profile in this zone is retained, with good accuracy, only in terms of the *average* (over this zone) frictional resistance.

(C) In the case of "fluctuating" $\tau(x)$, the propagation of sliding, at initial stages, is quite sensitive to the amplitude of the fluctuations (provided the average $\langle\tau\rangle$ is kept constant). However, at the point when the applied shear load σ^{∞}_{xy} reaches the average $\langle\tau\rangle$, this sensitivity is lost.

Statement A can be illustrated on the following two examples, that involve a local minimum and a local maximum of $\tau(x)$, respectively.

(1) *Propagation of sliding from an interval of local minimum of frictional resistance:* Propagation of sliding from the points of minimal frictional resistance, as a function of the shape of the minimum, is studied on three examples that model a drop of frictional resistance within a certain interval by three different shapes of $\tau(x)$: a triangle, a parabola and a step function (Fig. 6a). It is seen, from Fig. 6b, that the propagation rates have a substantial sensitivity to the shape: the propagation is noticeably slower for the triangular shape. An interesting observation is that the curves of Fig. 6a and b are similar (triangular/parabolic shapes of Fig. 6a correspond to the same shapes of Fig. 6b).

(2) *Propagation of sliding in the vicinity of a local maximum of frictional resistance:* We consider the case when the frictional resistance is increased (as compared to the constant background level τ_0) within a certain interval $(-l/2, l/2)$. This local maximum is modeled by three different shapes of $\tau(x)$: a triangle, a parabola and a step function. It is seen, from Fig. 7, that the propagation of sliding towards the point of maximal $\tau(x)$ is noticeably faster for the triangular shape.

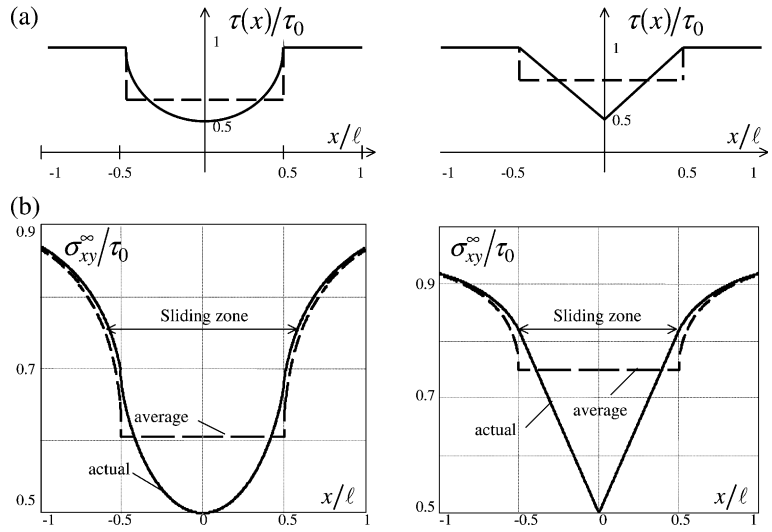

Fig. 8. Sensitivity of the sliding process to the replacement of the exact profile of local minimum of frictional resistance by its average (– – –). The sensitivity is quickly lost as the sliding zone extends beyond the interval of local minimum.

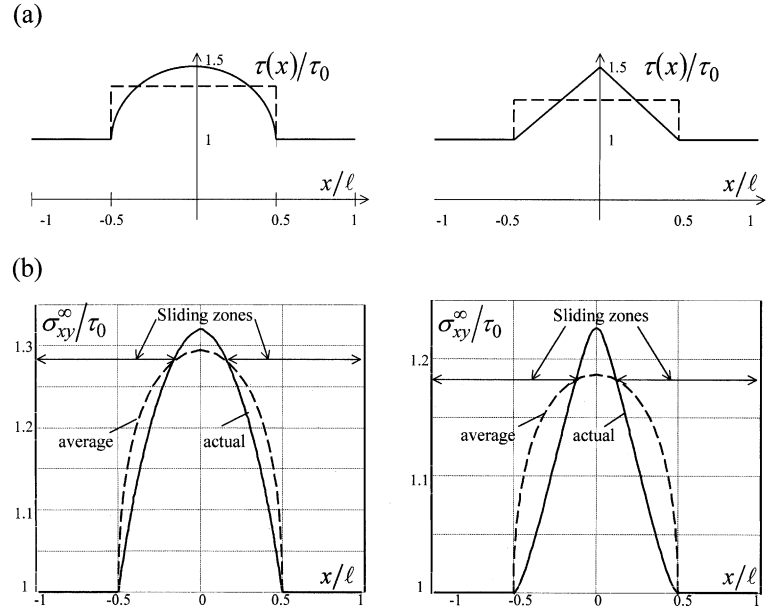

Fig. 9. Sensitivity of the sliding process to the replacement of the exact profile of local maximum of frictional resistance by its average (– – –).

Statement B can be illustrated as follows.

(1) In the case of *local reduction* of frictional resistance $\tau(x)$ within a certain interval, we replace the actual profile of $\tau(x)$ in this interval by its average over this interval. It is seen, from Fig. 8, that, after the interval has been slid, the curves that show the propagation of sliding for two shapes of $\tau(x)$ – circular and triangular – quickly merge with the ones corresponding to replacement of $\tau(x)$ by its average $\langle\tau\rangle$.

(2) We consider now the case of *elevated* level of frictional resistance $\tau(x)$ within a certain interval and examine the critical applied shear load σ_{xy}^{∞} at which the point of maximal $\tau(x)$ is crossed and two sliding zones coalesce. Analysis of the two shapes of a local maximum, shown in Fig. 9, indicates that, in the case of a "mild" maximum (circular shape), the replacement of $\tau(x)$ by $\langle\tau\rangle$ leads to only 2% reduction of the load at which the coalescence occurs; a somewhat "sharper" peak (triangular shape) leads to a larger reduction, of 4%. In this sense, the sensitivity to replacement of $\tau(x)$ by $\langle\tau\rangle$ is relatively weak (although it may increase for very sharp peaks of $\tau(x)$).

Statement C is illustrated in Fig. 10 on the example of the cosine profile of $\tau(x)$ with the average $\langle\tau\rangle = (1/2)\,\tau_0$. It is seen that, for larger amplitudes of $\tau(x)$ (and, thus, for "deeper" minimums), the sliding process initiates at lower σ_{xy}^{∞}. However, as σ_{xy}^{∞} reaches the level of $\langle\tau\rangle$, all the curves of Fig. 9b intersect, i.e. the zones of sliding coincide. As σ_{xy}^{∞} is raised above $\langle\tau\rangle$, the differences between the sliding zones corresponding to different amplitudes remain minimal. The differences in critical levels of σ_{xy}^{∞} at which the sliding zones coalesce are also small to moderate, for the range of amplitudes shown in Fig. 10a (although they will obviously increase, as the amplitude of $\tau(x)$ increases).

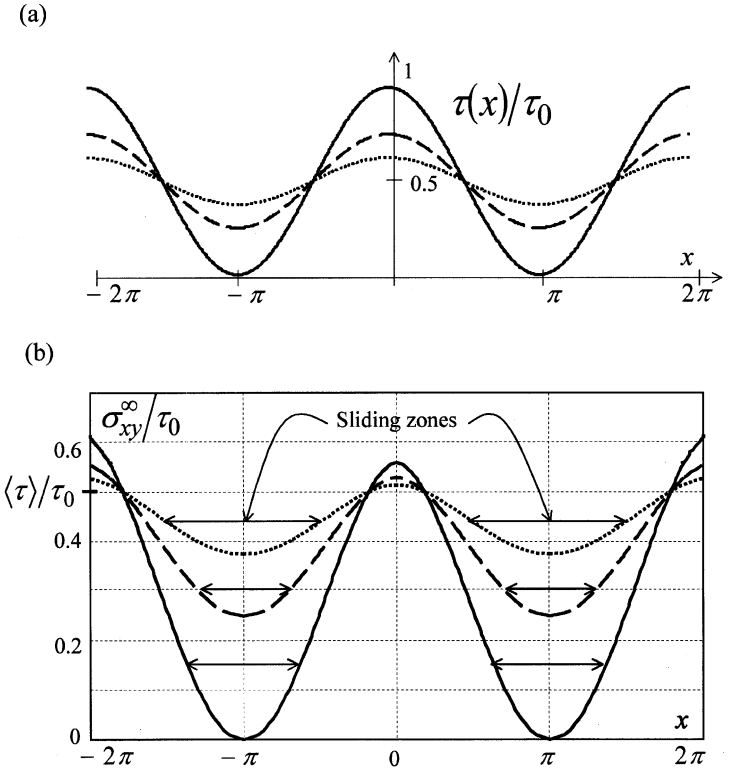

Fig. 10. Spatially fluctuating frictional resistance (modeled by a cosine curve). Propagation of sliding as a function of the amplitude.

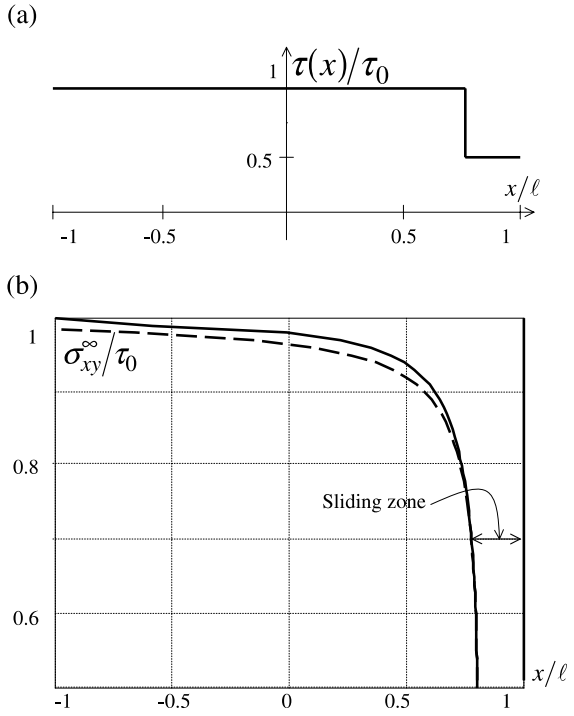

Fig. 11. Propagation of sliding after the sliding zone reaches one of the crack tips. (Dotted line indicates, for comparison, the case when the crack extends beyond the point $x = l$ and there is no effect of the crack tip.)

4.4. Propagation of sliding after the sliding zone has reached one of the crack tips

Until the sliding zone reaches one of the crack tips, the latter do not affect the sliding process, i.e. the process is the same as in the case of an infinite crack. (This is seen from the formulation of the problem, where the crack tips manifest themselves, in the form of inequality $K_{\mathrm{II}} < K_{\mathrm{IIC}}$, only when the sliding zone reaches one of them.)

As soon as one of the crack tips is reached, the propagation of sliding at the other end of the sliding zone slows down. This is illustrated in Fig. 11, on the example when $\tau(x)$ has a local minimum that is adjacent to the right tip of the crack. The solid line (the solution of the problem) is contrasted with the dashed line that corresponds to the case when $\tau = \tau_0$ on the right of $x = l$ (i.e. the crack expands beyond the point $x = l$ and there is no effect of the crack tip).

4.5. The effect of interaction between the sliding zones

The interaction between the sliding zones enhances the propagation of sliding. This is illustrated on two examples, each involving two sliding zones (initiating from two intervals of reduced τ).

The first example (Fig. 12) compares the process of sliding with two zones to the one involving only one sliding zone (dotted line). The enhancing effect of interaction is generally weak (the solid and the dotted lines are close), except for the last stage of propagation when the remaining ligament is small (this is related to the general weakness of crack interactions in the collinear arrangements). The enhancing effect of in-

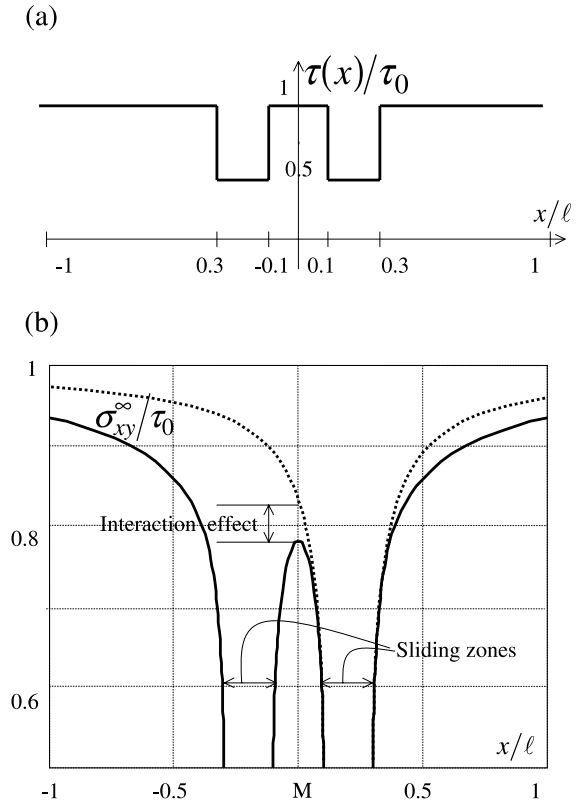

Fig. 12. Enhancing effect of interaction between two sliding zones of equal lengths. (Dotted lines indicate, for comparison, the solution for one sliding zone.)

teraction becomes noticeable at small spacings between the sliding zones; as a result, the magnitude of the applied stress σ^{∞}_{xy} at which the two zones coalesce (at the midpoint M), is 6% lower than the stress at which point M is reached by a *single* sliding zone, without the enhancing effect of the other zone.

The second example (Fig. 13) examines the effect of interaction as a function of the difference in sizes of the two sliding zones: the solid lines correspond to the ratio of the sizes 4:1 and the dotted lines to the ratio 1:1. (To make the effect of the size difference more explicit, we eliminated the influence of the crack tips, by assuming that the crack is sufficiently large.) As expected, the enhancing effect of a larger zone on a smaller one is stronger than vice versa.

5. Several collinear cracks undergoing frictional sliding

The analysis of sliding zones (their nucleation and propagation) on several collinear cracks is similar to the one for one crack, until one (or several) of the endpoints of the sliding intervals reaches one of the crack tips. After that, the fact that the line along which sliding takes place, incorporates several separate cracks, starts to affect the sliding process. Mathematically, this is due to the replacement of the condition $K_{\mathrm{II}} = 0$ at the endpoint(s) of the sliding zone(s) by the condition $K_{\mathrm{II}} < K_{\mathrm{IIC}}$.

The effect of the line of sliding being broken into several separate cracks is illustrated on the example of two cracks, the left one having low and constant value of τ and the right one having the profile of $\tau(x)$

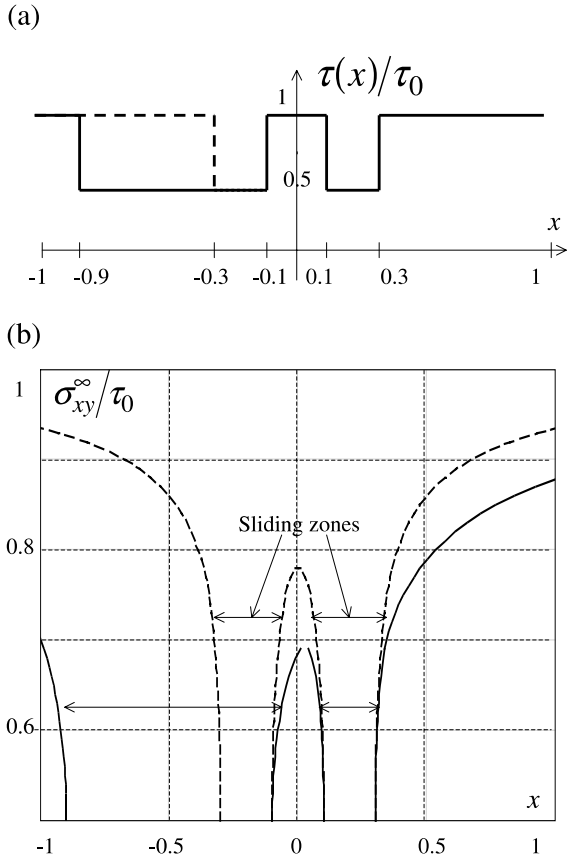

Fig. 13. Enhancing effect of interaction between two sliding zones of different lengths (ratio of lengths 4:1). Dotted line indicates, for comparison, the case of equal lengths.

shown in Fig. 14a. Frictional sliding initiates on the left crack (along its entire length). As the applied load σ^{∞}_{xy} is increased, sliding starts on certain intervals of the right crack. Sliding on the right crack is enhanced by the fact that the left crack has already slid. In Fig. 14b, the solid line (the solution of the problem) is contrasted with the dashed line that corresponds to the case when the left crack is absent. The enhancing effect of the left crack on sliding on the right crack is seen to be quite strong.

6. General solution in presence of open intervals

We now assume that, in addition to sliding intervals L_1 where Coulomb's law $\tau(x) = -\mu(x)\,\sigma_{yy} + c(x)$ holds, "open intervals" (collectively denoted by L_3) are present. By open intervals we mean the intervals (of given, fixed length) where tractions are equal to zero. They model situations where a part of a material has been lost (fell off) along a certain part of the crack. We emphasize that such traction free intervals are not caused by any system of "prying loads", but are fixed. In this respect, the problem is different from the one analyzed earlier by Comninou and Dundurs (1979, 1981) and Mendelsohn and Whang (1988).

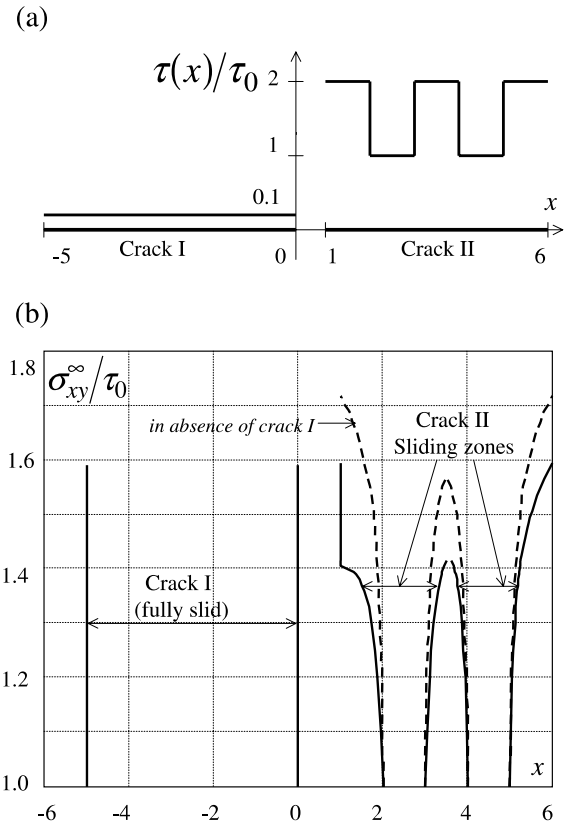

Fig. 14. Two cracks undergoing frictional sliding. Left and right cracks have uniform and piecewise constant frictional resistance, correspondingly (as indicated). Enhancing effect of the left crack on sliding on the right crack (dotted lines indicate, for comparison, the case when the left crack is absent).

Using the stress superposition of Fig. 15, we reduce the problem to two subproblems, as follows. Subproblem A involves mode I loading only, and traction σ^{A} along interval L_1 is given by the solution of the problem of an open interval under remote compression σ^{∞}_{yy} (and hence may have a singularity if the open interval has sharp tips). Subproblem B involves mode II only and it can be further decomposed into two subproblems: B1 and B2. Problem B2 can be solved by the method developed in Section 3, whereas the stress state in problem B1 is uniform shear σ^{∞}_{xy}.

Subproblem A is formulated as follows:

$$\begin{aligned} &\sigma^{\pm}_{yy}(x) = 0, \quad \sigma^{\pm}_{xy}(x) = 0, \qquad \text{for } x \in L_3 \\ &\sigma_{yy} \to \sigma^{\infty}_{yy}, \quad \sigma_{xx}, \sigma_{xy} \to 0 \qquad \text{at } z \to \infty \end{aligned} \tag{6.1}$$

We note, in connection with the superposition, that the following condition holds along the line L_1 in this subproblem (with the account of $\sigma_{xy} = 0$ on L_1):

$$\sigma_{xy}(x) + \mu(x)\,\sigma_{yy}(x) = \mu(x)\,\sigma^{\mathrm{A}}_{yy}(x), \quad \left[u_y\right] = 0, \qquad [\sigma_{xy}] = [\sigma_{yy}] = 0, \qquad \text{for } x \in L_1 \tag{6.2}$$

where $\sigma^{\mathrm{A}}_{yy}(x)$ is the stress generated along the line L_1 in this subproblem.

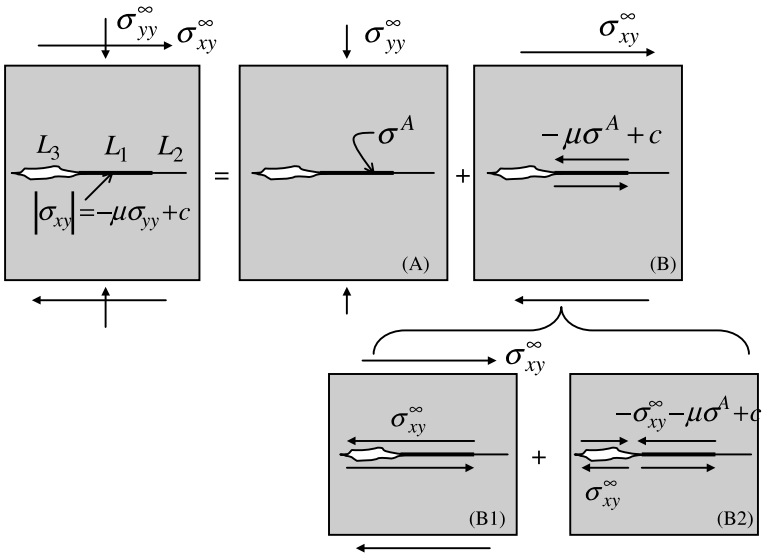

Fig. 15. Stress superposition in presence of open interval L_3.

Similarly, the subproblem B is formulated as follows:

$$\begin{aligned}
&\sigma^{\pm}_{xy}(x) = 0, \quad \sigma^{\pm}_{yy}(x) = 0 \qquad \text{for } x \in L_3 \\
&\sigma^{\pm}_{xy}(x) = -\mu(x)\,\sigma^{\mathrm{A}}_{yy}(x) + c(x), \quad \sigma^{\pm}_{yy}(x) = 0 \qquad \text{for } x \in L_1 \\
&\sigma_{xy} \to \sigma^{\infty}_{xy}, \quad \sigma_{xx}, \sigma_{yy} \to 0 \qquad \text{at } z \to \infty
\end{aligned} \tag{6.3}$$

with the following relation on L_1:

$$\sigma_{xy}(x) + \mu(x)\,\sigma_{yy}(x) = -\mu(x)\,\sigma^{\mathrm{A}}_{yy}(x) + c(x), \quad [u_y] = 0, \quad [\sigma_{xy}] = [\sigma_{yy}] = 0 \tag{6.4}$$

Adding up the right hand parts of Eqs. (6.2) and (6.4) recovers the original problem. Thus, the original problem is reduced to two Dirichlet's problems, on L_3 and on $L_1 \cup L_2$.

Remark 1. We note that the normal traction distribution σ^{A} depends on whether the endpoint of the open intervals is "sharp" or "blunted". We assume, in the analysis to follow, that the mentioned endpoints are sharp, so that σ^{A} involves a singularity generated at the tip of the open interval by the compressive loading (otherwise, σ^{A} has to be readjusted, in accordance with solutions for stress fields near slender notches).

Remark 2. Since σ^{A} enters the analysis only via product $\mu(x)\,\sigma^{\mathrm{A}}$, the singularity at the endpoints of the open interval can, formally, be attributed to $\mu(x)$ – these two physically different problems are mathematically identical. Thus, the problem with an open intervals can be reduced to the one considered in the preceding Sections, with singular $\mu(x)$.

Remark 3. A more general problem can be analyzed by similar means: instead of open intervals of zero traction, certain prescribed distributions $\sigma_*(x)$ and $\tau_*(x)$ of normal and shear tractions can be prescribed on L_3. Such a formulation may cover physically interesting situations, for example, the case of fluid pressure

applied along L_3. In this more general formulation, tractions $\sigma_*(x)$ and $\tau_*(x)$ will enter the analysis in a straightforward way: $\sigma^{\pm}_{yy}(x) = \sigma_*(x)$ for $x \in L_3$ in formula (6.1) and $\sigma^{\pm}_{xy}(x) = \tau_*(x)$ for $x \in L_3$ in formula (6.3).

We now consider several examples that illustrate the effect of open intervals.

7. Analysis of sliding process in presence of open intervals

We show that open intervals, generally, hinder the sliding process, except for the case (Example A) when the friction coefficient $\mu = \text{const}$ outside of the open interval (in which case the open interval has no effect on sliding). In order to reduce the number of parameters, we set cohesion coefficient $c = 0$ in Examples A–C, although the developed method, generally, accounts for the cohesion coefficient $c = c(x)$.

Example A. Frictional coefficient $\mu = \mu_0$ outside of the open interval $(-a, a)$. Sliding starts at points x where condition (2.1a) is satisfied; in this particular example this condition is as follows:

$$\sigma_{xy}(x) + \mu_0 \sigma_{yy}(x) = 0 \tag{7.1}$$

where σ_{yy} and σ_{xy} are stresses on L_1 (in presence of the open interval). We assume that the endpoints of the open interval are sharp, so that σ_{yy} and σ_{xy} involve a singularity generated at the tips of the open interval:

$$\sigma_{yy} = \frac{\sigma^{\infty}_{yy}|x|}{\sqrt{x^2 - a^2}}, \qquad \sigma_{xy} = \frac{\sigma^{\infty}_{xy}|x|}{\sqrt{x^2 - a^2}} \tag{7.2}$$

Substituting Eq. (7.2) into Eq. (7.1) leads to cancellation of singular multipliers at the normal and shear terms, so that the condition of nucleation of sliding is re-stated simply as $\sigma^{\infty}_{xy} + \mu_0 \sigma^{\infty}_{yy} = 0$. Its satisfaction occurs at all points x simultaneously and sliding takes place along the entire crack. Note, that this conclusion also applies to the case when the open interval is located asymmetrically with respect to the crack center, including the limiting case when it is adjacent to one of the crack tips.

Since the condition of sliding in this case coincides with the one in absence of the open interval, the presence of an open interval produces no effect on the initiation of sliding. This physically interesting observation holds also in a more general case of several open intervals.

Example B. The friction coefficient is piecewise constant outside of the open interval (Fig. 16a).

Applying the same condition (7.1) yields that sliding starts at $\sigma^{\infty}_{xy} = \mu_1 \sigma^{\infty}_{yy}$ along the entire length of the intervals $a < |x| < b$. Further increase of σ^{∞}_{xy} leads to a gradual propagation of sliding into intervals $|x| > b$ of higher μ. As follows from the superposition of Fig. 15, this problem reduces to the one with one sliding zone $(-h, h)$, with the following traction distribution (Fig. 17):

$$\sigma_{xy} = \begin{cases} \sigma^{\infty}_{xy}, & |x| < a \\ \sigma^{\infty}_{xy} - \mu(x) \frac{\sigma^{\infty}_{yy}|x|}{\sqrt{x^2 - a^2}}, & |x| > a \end{cases} \tag{7.3}$$

Endpoints $\pm h$ of the sliding zone are found from the condition $K_{\mathrm{II}}(\pm h) = 0$ that yields:

$$\frac{\sigma^{\infty}_{xy}}{\sigma^{\infty}_{yy}} = \mu_2 - \frac{2}{\pi}(\mu_2 - \mu_1) \arctan \sqrt{\frac{b^2 - a^2}{h^2 - b^2}} \tag{7.4}$$

For comparison, consider the case when the open interval is absent (and is replaced by the sliding interval of $\mu = \mu_1$). Then, Eq. (7.4) is to be replaced by

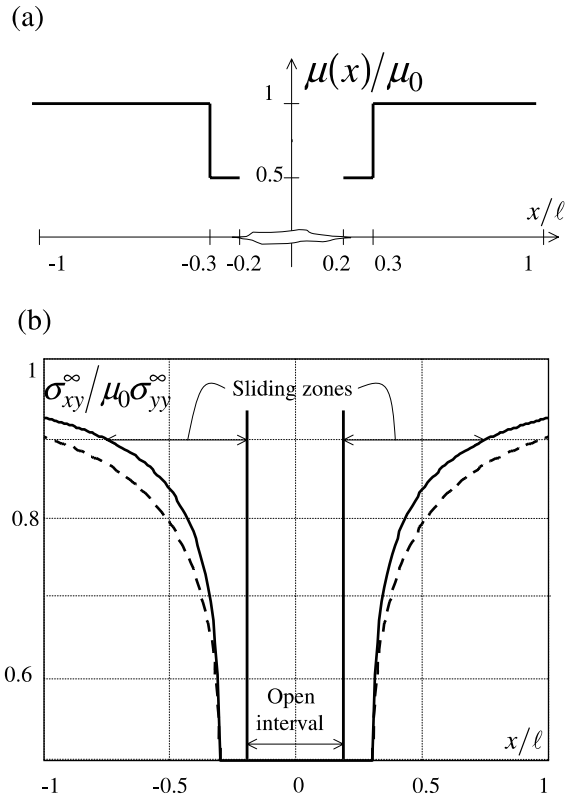

Fig. 16. Open interval surrounded by a piecewise constant profile of frictional resistance. Propagation of the sliding zone as σ^{∞}_{xy} increases. Dotted line indicates, for comparison, the case when the open interval is replaced by an interval with $\mu/\mu_0 = 0.5$.

$$\frac{\sigma^{\infty}_{xy}}{\sigma^{\infty}_{yy}} = \mu_2 - \frac{2}{\pi}(\mu_2 - \mu_1)\arcsin\frac{b}{h} \tag{7.5}$$

Comparison of the two results (Fig. 16b) shows that the presence of an open interval in the midst of the sliding zone hinders the propagation of sliding. Physically, this effect may be explained by the fact that, in the considered case, the presence of an open interval generates singular compressive stresses at its tips (whereas shear stresses remain non-singular there).

Example C. We examine the effect of the crack tip, by modifying Example B: the open interval is adjacent to the crack tip $x = -a$. A similar analysis, based on the condition $K_{\mathrm{II}}(h) = 0$, yields to following equation for the right endpoint h of the sliding zone as a function of applied loads:

$$\frac{\sigma^{\infty}_{xy}}{\sigma^{\infty}_{yy}} = \frac{\mu_1 a + \mu_2 \ell}{a + \ell} + \frac{2(\mu_2 - \mu_1)}{\pi(a + \ell)}\left[\sqrt{(b - a)(\ell - b)} + a\arcsin\frac{\ell + a - 2b}{\ell - a} - (\ell - a)\arctan\sqrt{\frac{b - a}{\ell - b}}\right] \tag{7.6}$$

Comparison with Example B shows, that having a crack tip as one of endpoints of the open interval hinders, to some extent, the propagation of sliding.

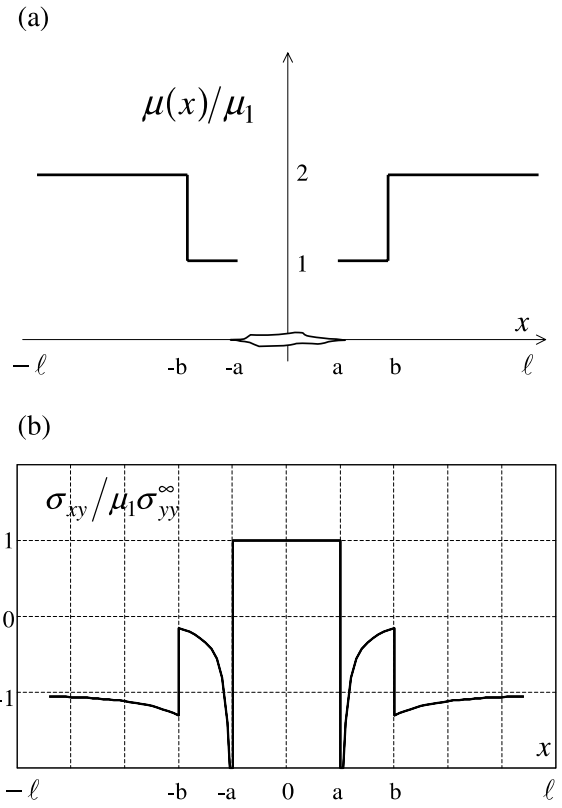

Fig. 17. Shear traction distribution in the problem with an open interval.

8. Displacement discontinuity profile along the crack line

We now analyze the distribution of displacement discontinuity (the accumulated slip displacement) along the sliding contact. This problem is relevant for geomechanical applications where, for example, the fault slip distribution may be of interest (Schultz, 1999).

The displacement discontinuity along the crack faces can be found from Eq. (3.1a):

$$\left[u_x^+ - u_x^-\right](\xi) = \frac{\kappa+1}{2\mu}\left(\int_{a_i}^{\xi}\frac{1}{\pi i X(x)}\int_L \frac{X(t)\,\sigma_{xy}(t)\mathrm{d}t}{t-x}\mathrm{d}x + 2\int_{a_i}^{\xi}\frac{P_n(x)}{X(x)}\mathrm{d}x\right) \tag{8.1}$$

where μ is Lame's constant and where $\kappa = 3-4\nu$ for plane strain, $\kappa = (3-\nu)/(1+\nu)$ for generalized plane stress and L_1 may, generally, comprise several sliding intervals: $L = \cup(a_k, b_k)$. Expressions for $X(x)$ and $P_n(x)$ are given by Eqs. (3.3) and (3.4), respectively, and "driving force" $\sigma_{xy}(x)$ is as follows:

$$\sigma_{xy}(x) = \sigma^{\infty}_{xy} - \tau(x), \quad x \in L_1 \quad \text{in absence of open intervals} \tag{8.2}$$

$$\sigma_{xy}(x) = \begin{cases} \sigma^{\infty}_{xy}, & x \in L_3 \\ \sigma^{\infty}_{xy} + \mu(x)\,\sigma^{\mathrm{A}}_{yy} - c(x), & x \in L_1 \end{cases} \quad \text{in presence of open intervals} \tag{8.3}$$

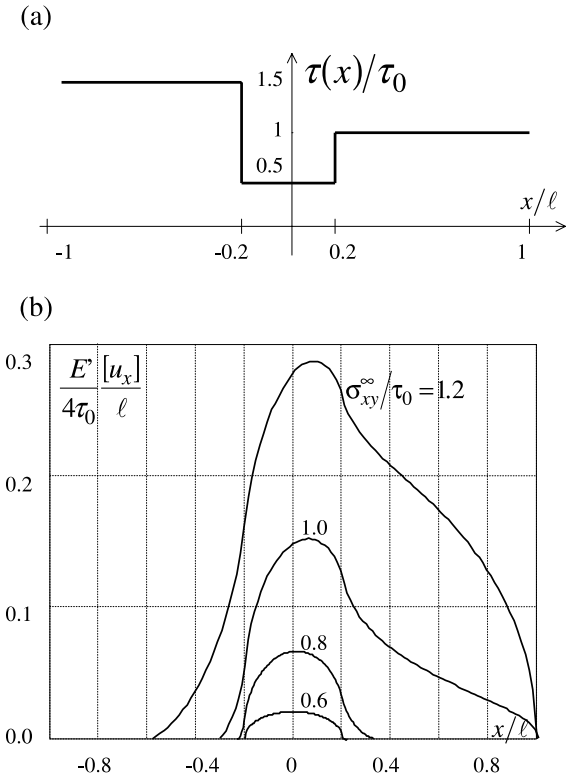

Fig. 18. Slip distribution at increasing σ_{xy}^{∞}. The case of piecewise constant frictional resistance (E' equals to Young's modulus E in plane strain and to $E/(1-\nu^2)$ in plane stress).

We now consider two representative examples.

(1) *Piecewise constant frictional resistance in absence of the open intervals (Fig. 18a):* Fig. 18b illustrates the slip distribution (corresponding to the same numerical parameters as in the example of Section 4.2), at different levels of applied σ_{xy}^{∞}. An interesting observation is that the peak in the displacement discontinuity moves to the right, as σ_{xy}^{∞} increases; this is due to asymmetry of the profile of frictional resistance. Thus, the mentioned peak moves away from the point where the sliding started. This result may be relevant to some observations on slip distribution along geological faults (Schultz, 1999).

We also note that there are two inflection points in the slip profiles. They are caused by discontinuities of the frictional resistance and move in the process of sliding propagation, as seen from Fig. 18b. After the sliding zone reaches one of the crack tips, the effect of the latter on the slip distribution becomes quite significant, as seen from the same figure.

(2) *An open interval is present with piecewise constant frictional resistance outside of it (Fig. 19a):* Fig. 19b illustrates the corresponding slip distribution considered at different levels of applied shear load σ_{xy}^{∞}. In this case, sliding is preceded by a "deadband" – an interval of loads where no sliding occurs (although the tangential displacement discontinuity, of the elliptical shape, does occur along the open interval). Interesting observations are that the shape of the discontinuity within the open interval remains elliptical, and that the profile has inflection points at the points of discontinuity of $\mu(x)$.

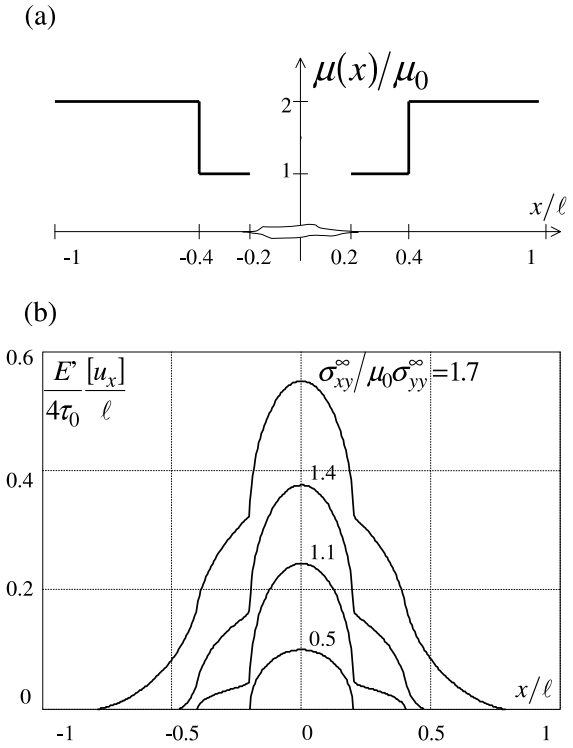

Fig. 19. Slip distribution in presence of an open interval at increasing σ^{∞}_{xy}. The case of piecewise constant frictional coefficient (E' equals to Young's modulus E in plane strain and to $E/(1-\nu^2)$ in plane stress).

9. Discussion and conclusions

The problem of frictional sliding on one or several collinear cracks, with non-uniform frictional resistance $\tau(x)$ along the crack faces is analyzed. The frictional resistance may be specified by Coulomb's law: $\tau(x) = -\mu(x)\sigma_{yy} + c(x)$, but this is not a necessary restriction for our analysis.

Three different regimes may take place along the crack: frictional sliding, locked state and open, traction free intervals that may model the situations when a part of the material fell off from the crack zone (note that the condition of zero tractions on the open interval can actually be generalized to the condition of prescribed tractions there). As the applied remote shear loading is increased, sliding starts at the point(s) of the lowest frictional resistance and then propagates; in the case of several sliding intervals, the latter interact with each other, producing a mutually enhancing effect. Similar enhancing effect is produced by the interaction of slidings on several collinear cracks.

The sensitivity of the sliding process to the exact profile of frictional resistance $\tau(x)$ (or, to the distribution $\mu(x)$ of the frictional coefficient if Coulomb's law is assumed) is examined. Such an analysis is of importance because the frictional characteristics can usually be estimated in a very approximate way. The basic findings can be summarized as follows. In the case of a local minimum of $\tau(x)$ within a certain interval, the propagation of sliding is, initially, quite sensitive to the "details" of the profile of $\tau(x)$. However, after the interval of reduced $\tau(x)$ has been slid and "left behind", further propagation of sliding loses sensitivity to the "details": it is almost unaffected by the replacement of $\tau(x)$ in the mentioned interval by its average (over this interval) value $\langle\tau\rangle$.

Until the sliding zone has reached one of the crack tips, the latter do not affect the sliding process (i.e. the process does not depend on the crack length). After one of the tips has been reached, further propagation of sliding (at the other end of the sliding zone) is slowed down, although this effect is relatively mild.

An interesting finding is that the presence of open intervals (that simulate the situations when part of the material fell off) hinders the propagation of sliding. This may be explained by the fact that such intervals may generate singularities of compressive stress at their endpoints (whereas the shear stress remains non-singular there, due to the condition $K_{II} = 0$).

The slip distribution over the non-uniformly sliding crack is examined on two representative examples (with and without an open interval). An interesting finding is that, as sliding progresses, the point of the maximal slip may move away from the point where the sliding started. This finding may be relevant to certain observations on slip distribution along geological faults.

Acknowledgements

This research has been supported by the National Science Foundation through grant to Tufts University. The first author (L.G.) acknowledges support of Zonta International Amelia Earhart Fellowship Award.

References

Comninou, M., Dundurs, J., 1979. An example for frictional slip progressing into a contact zone of a crack. Engng. Fract. Mech. 12, 191–197.

Comninou, M., Dundurs, J., 1981. An educational elasticity problem with friction. Part 1: loading, and unloading for weak friction. J. Appl. Mech. 48, 841–845.

Comninou, M., Dundurs, J., 1983. Spreading of slip from a region of low friction. Acta Mechanica 47, 65–71.

Cooke, M., 1997. Fracture localization along faults with spatially varying friction. J. Geophys. Res. 102 (B10), 22425–22434.

Mendelsohn, D., Whang, K., 1988. Partial release and relocking of a frictionally locked crack due to moving tensile loads. J. Appl. Mech. 55, 383–388.

Muskhelishvili, N.I., 1953. Some Basic Problems in the Mathematical Theory of Elasticity. Noordhoff, Groningen.

Olsson, W., 1984. A dislocation model of the stress history dependence of frictional slip J. Geophys. Res. 89 (B11), 9271–9280.

Pollard, D., Segall, P., 1980. Mechanics of discontinuous faults. J. Geophys. Res. 85 (NB8), 4337–4350.

Schultz, R., 1999. Understanding the process of faulting: selected challenges and opportunities at the edge of the 21st century. J. Struct. Geology 21 (8–9), 985–993.

Weertman, J., 1964. Continuum distribution of dislocations on faults with finite friction. Bull. Seis. Soc. Amer. 54 (4), 1035–1058.